Supporting Information

Template Synthesis of Cyanine Dye H-aggregates on Nano-structured [6,6]- Phenyl C_{61}-Butyric Acid Methyl Ester Substrates

Jakob Heier,* Rolf Steiger, Roland Hany and Frank Nüesch

BET adsorption isotherm

   We applied several models adapted from the isotherm models to analyze monomer and dimer film formation. As a first feasibility test, we investigated the monomer adsorption of the dye Cy3-I as a function of the solution concentration for two different substrates, a plain PCBM film and a PCBM template surface (Supplementary Figure 1a). Both curves have a similar convex shape for low concentrations (similar to BET-isotherms of type II), indicating strong interactions between adsorbent and adsorbate and negligible interaction between the dye molecules. The concave shape for low concentrations in Figure 4b is misleading, it is only a consequence of the logarithmic presentation. As we do not find any evidence for dimerization in the liquid spectroscopically, we only considered the equilibrium between the monomer in solution and the monomer on the substrate surface. The film formation on the plain PCBM films follows an exponential growth behavior (equation 1), while we find an amazing agreement between the experimental data and a model derived from the BET model (equation 2) for the template surface (Supplementary Figure 1a, Supplementary Table 1). From the

BET-model, we adopt a solubility concentration c_{sat} of the dye and the attenuance $ATT_{m,0}$ that defines a plateau attenuance (equation 2). In the BET model the plateau originates from monolayer coverage of the substrate, in our case the plateau is defined by the onset of H-aggregation.

$$ATT_m \propto [C]^n \qquad (1)$$

$$ATT_m = \frac{K \times ATT_{m,0} \times [C]}{(C_{sat} - [C]) \times (1 + (K-1) \times [C]/C_{sat})} \qquad (2)$$

Furthermore, in equations (1) and (2), ATT_m is the attenuance of the monomer in the film, $[C]$ is the dye concentration in solution, n a critical exponent, K the equilibrium constant between adsorbed dye and the dye in solution. The fitting parameters, including the correlation R^2, for the 4 dyes studied are summarized in the Supplementary Table 1, the critical exponent for Cy3-I on a flat PCBM substrate is n = 0.7. We were not able to identify isosbestic points in the adsorption spectra, thus questioning a further analysis of the data with respect to eventually existing equilibria between monomers and dimers on the PCBM surface. Surprisingly, the dimer adsorption can also be described by equation 2, suggesting also dimer adsorption from solution.

The meaning of the values obtained from the fitting routine should not be over-emphasized. Even though the values for C_{sat} strictly follow the solubilities of the dye, the attenuances at H-aggregation onset $Att_{m,0}$ differ significantly and we do not have a clear rationale for this. Note that we also introduce a systematic error by plotting the overall dye concentration instead of monomer and dimer concentrations on the x-axis in Figures 5a, b.

PCBM sub-cluster diameter and Mie-scattering spectrum

To establish a relation between PCBM sub-cluster diameter and Mie scattering spectrum, an analysis of the PCBM cluster size distribution within one sample is necessary. This proved to be difficult with the PCBM original template films, since the PCBM domains are curved, eventually show multi-layers of sub-clusters and the sub-clusters are often not clearly separated. Therefore, we utilized the same liquid-liquid dewetting process with solutions of different compositions to generate morphologies where PCBM clusters of corresponding size formed only in a single layer and were well-separated from each other. The PCBM clusters form inside dewetting holes of a continuous PCBM film (Supplementary Figure 2a, b). Similar to the PCBM template films, the PCBM clusters here also cause Mie-scattering (Supplementary Figure 2d), and diameters and domain size distributions as analyzed by SFM are shown in Supplementary Figure 2c. The domain area histogram and the Mie-scattering spectrum have qualitatively the same shape, and smaller mono-disperse PCBM clusters give raise to a sharp Mie-scattering peak at smaller wavelength, while larger PCBM clusters with a broad size distribution give raise to a broader Mie-scattering spectrum at higher wavelength. From the peak wavelength a relation between Mie-peak position and PCBM sub-cluster size could be established (Supplementary Figure 2e).
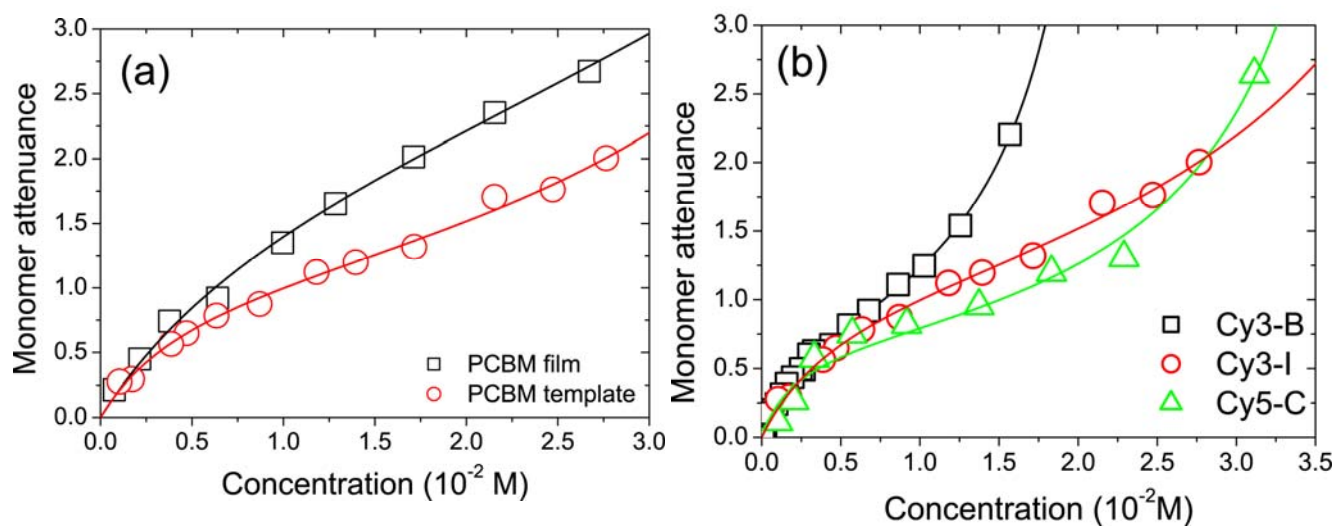
Supplementary Figure 1. (a) Monomer peak attenuance vs. solution concentration (adsorption isotherms) of the dye Cy3-I on a flat PCBM surface and a template surface. (b) Monomer attenuance vs. solution concentration of three different dyes on a templating surface. The solid lines are fits to the experimental data using eq 1 (PCBM film) and eq 2 (PCBM template). The fitting parameters are summarized in Supplementary Table 1.
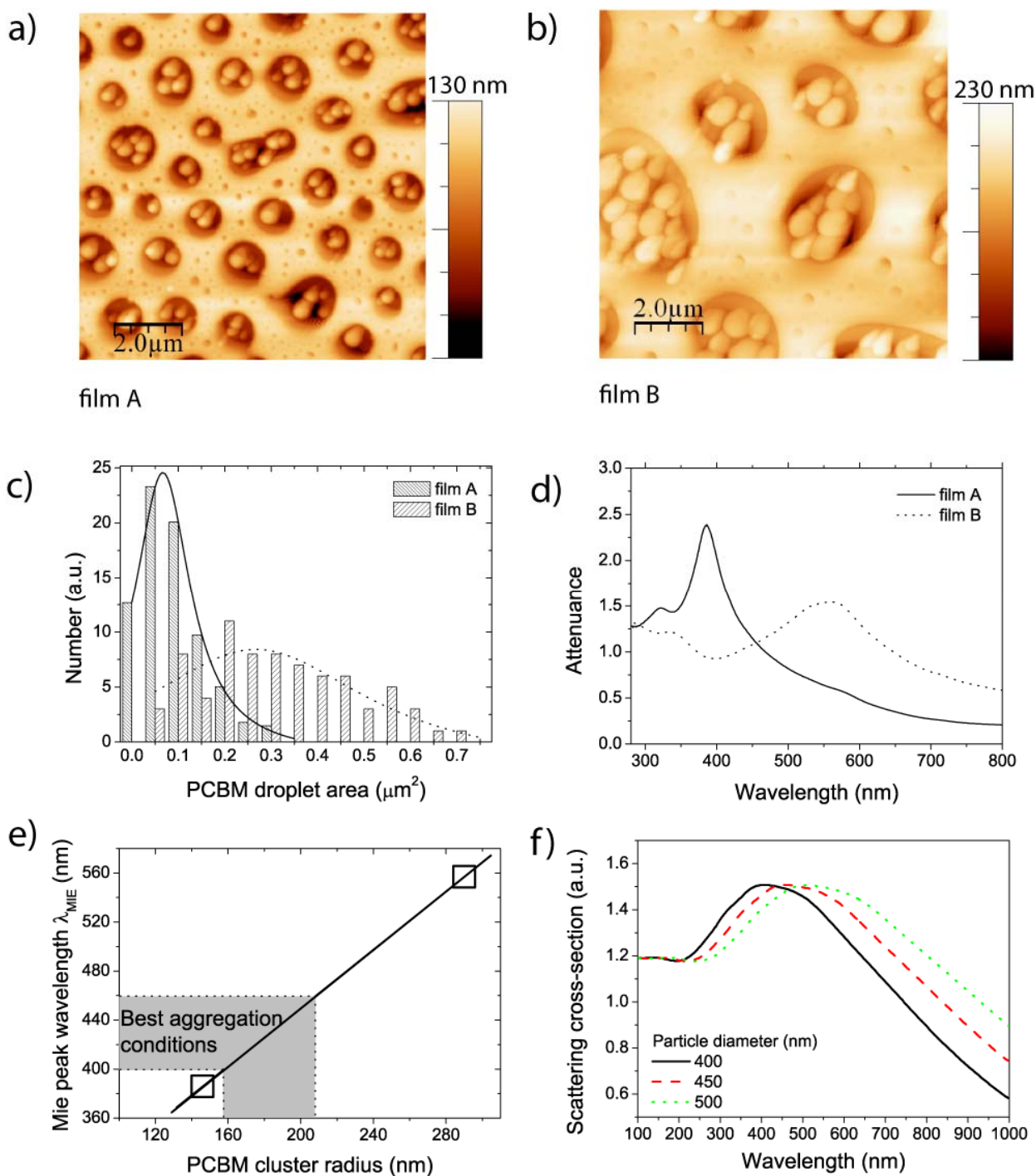
Supplementary Figure 2. (a, b) SFM images of PCBM - Cy3-C blend films. PCBM forms individual sub-clusters in a dewetting PCBM film. (c) Area size distributions of the PCBM sub-clusters from films A and B. For the analysis, a much larger sample set has been used. The histogram is normalized with respect to the total number of clusters. (d) Attenuance spectrum of film A and film B. (e) Combining

Supplementary Figure 1c and Supplementary Figure 1d, a relation between the Mie-scattering features and the PCBM sub-cluster area size distribution can be established. (f) Simulation of the Mie-scattering cross section of particles of different diameters. We chose an index of refraction of 1.6 and 0.3 (real and imaginary part, respectively). The simulation demonstrates the sensitivity of the peak scattering wavelength to the dimension of the scattering particles. Mie scattering simulations were done with the program MieCalc of Simuloptics GmbH (Germany).

Supplementary Table 1. Solubility c_{sat}, attenuance $ATT_{m,0}$ for H-aggregation onset and adsorption constant K obtained from fitting the adsorbances to eq 2.

Dye	c_{sat} (10^{-2} M)	$ATT_{m,0}$	K	Correlation R^2
Cy3-I-Monomer	5.9	1.16	12.1	0.9938
Cy3-I-Dimer	7.2	1.38	16.4	0.9841
Cy3-B-Monomer	2.4	0.82	10.8	0.9973
Cy3-B-Dimer	2.7	0.99	12.6	0.9946
Cy3-C-Monomer	5.4	1.31	21.1	0.9877
Cy5-C-Monomer	4.2	0.70	20.2	0.9808